Astronomy & Astrophysics manuscript no. April 14, 2003
(DOI: will be inserted by hand later)

Direct spectroscopic analysis of SN1999aa

G. Garavini[1], G. Folatelli[1], A. Goobar[1],S. Nobili[1],P. Nugent.....

Department of Physics, Stockholm University,
SCFAB, S–106 91 Stockholm, Sweden

Abstract. We present a detailed analysis of the peculiar Type Ia supernova SN1999aa in NGC 2595. This supernova has been suggested as a possible link between peculiar over-luminous and *Branch normals*. Our data set includes 25 optical spectra between -11 and +58 days with respect to B-band light curve maximum. We compare the observations with synthetic SYNOW spectra. In the early epochs, evidence is found for carbon at high and photospheric velocities and for highly ionized ions. Thus, the derived atmosphere properties soon after the explosion are consistent with the expectations for a high temperature unburned C+O rich region.
The first clear sign of SiII λ6355 Å characteristic for Type Ia supernovae, is found at day -7. The velocity range for this line and its time evolution indicate that the absorption is confined to a thin detached layer. We note a similar behavior for SN1991T, SN1997br and SN2000cx. The implications for supernova hydrodynamical models are discussed briefly.

1. Introduction

The apparent homogeneity of the brightness of Type Ia supernovae (SNe) has become an excellent tool for distance estimates. The intrinsic spread in their absolute B magnitude is less than 0.4 mag and it can be corrected through empirical correlations to be as good as 0.14 mag (Phillips et al., 1999), making high redshift Type Ia SNe a powerful tool for the determination of cosmological parameters (Goobar & Perlmutter, 1995; Perlmutter et al., 1999; Riess et al., 1998).

Cosmological implications derived from supernovae rely on the assumption that distant SNe explosions are mere copies of the better known nearby ones. The increasing number of high quality data-sets of low redshift supernovae is shedding new light on the big and small diversities found among these objects. Studying and understanding the (in)homogeneity within the Ia class of SNe is of vital importance to pursue precision cosmological measurements and to clarify issues like brightness evolution effects and classification of peculiar supernovae.

With this goal the SCP coordinated an extensive campaign for finding a large number of nearby Type Ia supernovae and to obtain extensive follow-up observations during the spring of 1999, (Aldering , 2000; Nugent & Aldering, 2000). The subject of this work, SN1999aa, was followed in this campaign and has been discussed as a very interesting object by several authors (Branch, 2000; Branch et al., 2001; Li et al., 2001b). It has been proposed as a key object to connect the peculiar over-luminous Type Ia SNe (SN1991T-like) to the 'Branch-normal', which may

Send offprint requests to: G. Garavini , gabri@physto.se

help in understanding the physical origin of the observed diversities. The paper is organized as follows. The spectroscopy data of SN1999aa and a short description of the data reduction scheme are presented in section 2. An introduction on supernovae theory and modeling is given in section 3. A detailed description of the spectra time sequence is given in section 4 where we present a detailed comparison of SN1999aa spectra with public data of spectroscopically peculiar and normal supernovae. The analysis of the velocities inferred from several spectral features are shown and discussed in section 5. Synthetic spectra produced with the highly parametrized SYNOW code are explored in section 6 and our final considerations about supernovae models and physics are given in section 7 and 8.

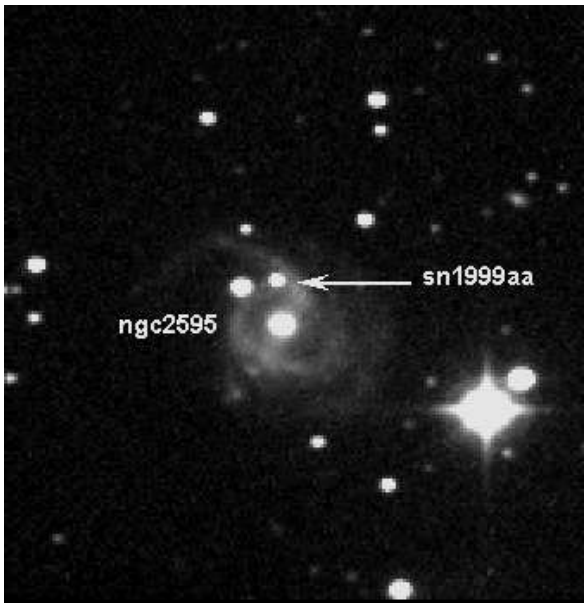

Fig. 1. SN1999aa in its host galaxy NGC 2595. R.A. = $8^h27^m42^s.03$, Decl. = $+21^o29'14".8$ (equinox 2000.0).

2. Data and data reduction

Arbour (1999), Qiao et al. (1999) and Nakano et al. (1999) reported the discovery of SN1999aa in the galaxy NGC 2595 measuring its position as R.A. = $8^h27^m42^s.03$, Decl. = $+21^o29'14".8$ (equinox 2000.0) on an unfiltered CCD image taken on Feb. 11.0166 UT. Filippenko et al. (1999) noted that it was a 91T-like peculiar Type Ia supernova based on a spectrum on February the 12th . Fig. 1 shows the position of SN1999aa and its host galaxy. NGC 2595 is a SBc type with a compact blue core and blue spiral arms at redshift $z = 0.0146$ (The recession velocity of the host galaxy, determined from narrow H-alpha and [N II] emission, is 4485 km/s). Based on the Schlegel et al. (1998) model the reddening due to the milky way for SN1999aa is $E(B-V) = 0.04$ mag as reported by Krisciunas et al. (2000) that also estimated a negligible host galaxy reddening. The SCP campaign follow up of this supernova consists in 25 different optical spectra ranging between 11 before and 58 days after maximum (in the following of this work the epoch will be given with respect to the maximum B light) using 5 different instruments. Specifications of the data set are provided in Tab. 1 and the spectral time sequence is shown in Fig. 2. All the raw data were analyzed with a common reduction scheme using standard IRAF routines. The two-dimensional images were bias-subtracted and flat-fielded using calibration images taken with the same instrument setting as the SN spectra and during the same night of observation. The sky background subtraction was performed on the resulting images using a fitted model of the sky and the sky spectrum itself was extracted for further checks on the wavelength calibration. The supernova spectrum was then extracted using the variance weighted optimal aperture extraction method (Horne , 1986). During the observations several arc lamp exposures were taken in order to calculate the dispersion solution and convert the pixel scale to wavelength for each given night. An atmospheric extinction correction was applied using a tabulated average extinction provided by the observatory. The accuracy of the calibration was checked against sky lines and generally found to be consistent within 2 Å . Spectrophotometric standard

JD -2400000	Epoch ref B_{max}	Telescope	Instrument	λ Region Å
51223.38	-11	NOT 2.6m	ALFOSC	3014-8972
51223.38	-11	NOT 2.6m	ALFOSC	3865-10032
51231.35	-3	NOT 2.6m	ALFOSC	2990-8857
51231.35	-3	NOT 2.6m	ALFOSC	3900-10025
51234.71	-1	Lick 3m	KAST	3279-5430
51234.71	-1	Lick 3m	KAST	5019-10474
51239.68	+5	MDM 2.4m	MARK III	3871-8806
51239.68	+6	MDM 2.4m	MARK III	3870-8808
51247.63	+14	APO 3.5m	DIS	3627-5887
51247.63	+14	APO 3.5m	DIS	4865-10333
51253.37	+19	NOT 2.6m	ALFOSC	2963-8862
51253.39	+19	NOT 2.6m	ALFOSC	3879-9994
51258.51	+25	CTIO 4m	RCSP	3210-9208
51261.54	+28	CTIO 4m	RCSP	3238-9237
51261.54	+28	CTIO 4m	RCSP	3238-9237
51266.53	+33	CTIO 4m	RCSP	3217-9199
51266.53	+33	CTIO 4m	RCSP	3217-9199
51273.62	+40	APO 3.5m	DIS	3616-5877
51273.62	+40	APO 3.5m	DIS	4860-10330
51282.67	+47	Lick 3m	KAST	3304-5462
51282.67	+47	Lick 3m	KAST	5003-10429
51286.63	+51	APO 3.5m	DIS	3615-5874
51286.63	+51	APO 3.5m	DIS	4863-10325
51293.71	+58	Lick 3m	KAST	3251-5390
51293.71	+58	Lick 3m	KAST	5214-7962

Table 1. Data set specification.

stars were observed during each night and were used to flux calibrate the SN spectra. A comparison between observation of different standard stars during the same night is used to check for possible systematic errors. In most of the cases the total exposure time was divided in different exposures in order to allow the elimination of the effect of cosmic rays on the final spectrum. A correction for Milky-Way extinction was applied using the standard procedure in (Cardelli et al., 1989) and assuming $R_V = 3.1$. Finally, the host galaxy spectrum was subtracted. No corrections for the telluric lines or for residual fringing patterns were performed. For a complete description of the data reduction methodology see (Folatelli et al., 2003a).

3. Models for Type Ia SNe

The most widely accepted model for Type Ia supernovae incorporates a degenerate C+O white dwarf (WD) accreting material through an overflow from a companion star.

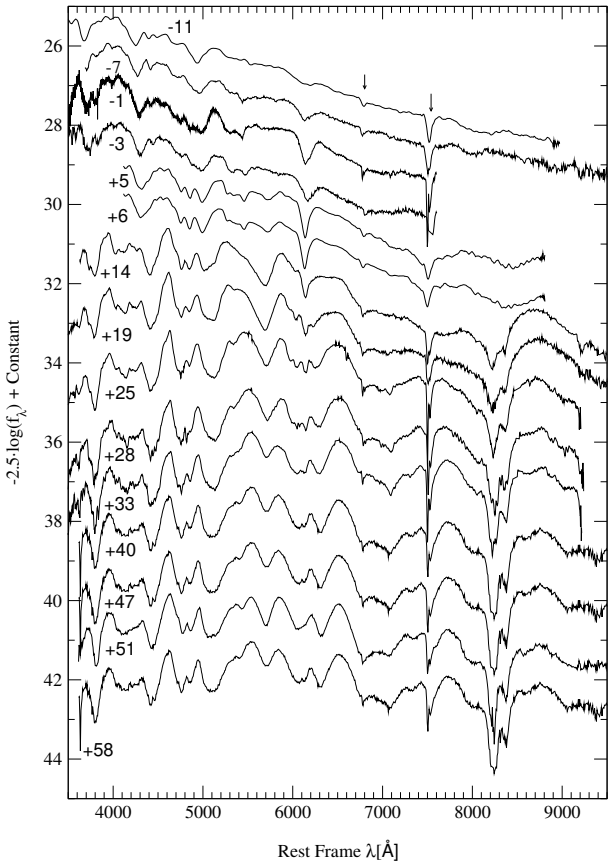

Fig. 2. SN1999aa spectral time sequence. The epochs are referred to B-band maximum light. The two arrows mark the uncorrected atmospheric absorptions

As the mass of the WD exceeds the Chandrasekhar limit the object starts contracting resulting in a compression of the star core and to an increasing of the central temperature that triggers thermonuclear reactions. The energy so released increases the temperature and consequently accelerate the thermonuclear reactions. Convective and conductive neutrino cooling work in slowing down the nuclear process, the net effect however eventually results in a rise of the central temperature leading to the expansion of the burning material (thermonuclear runaway). The density at which the ignition starts is thought to depend on the accretion history of the WD. Fast accretion produces higher central temperatures and lower ignition densities. Most of the energy released during the explosion is due to the explosive burning of carbon and oxygen, thus the energy produced depends strongly on the initial composition of the WD. A major part of the energy production occurs in a thin flame propagating outwards. Carbon and oxygen burning proceeds then toward the external layers subsonically (*deflagration*) (Nomoto et al., 1984). The innermost layers are then burned completely to statistical equilibrium composition (NSE) forming the iron-peak core of the supernova. The energy produced during the thermonuclear burning fuels the expansion but not the luminosity that it powered up by the radioactive decay ^{56}Ni$\rightarrow^{56}$Co$\rightarrow^{56}$Fe. To match the observed intermediate mass elements (IME) composition, the models require the burning front to accelerate and reach the external layer. The local densities and temperature of the external layers are too low for the nuclear burning to be complete. Incomplete Si-burning and unburned C+O compositions are then present in the outermost layers. In the delayed detonation hydrodynamical models the deflagration phase is followed by a supersonic burning period, (*detonation*) (Khokhlov, 1991; Yamaoka et al., 1992; Woosley et al., 1986). The deflagration to detonation transition (DDT) is usually parameterized by the transition density ρ_{tr}. The lower ρ_{tr} the less ^{56}Ni is produced and the intermediate mass elements are produced at lower external radii because of a shorter pre-expansion phase. The same effect is produced by a lower C/O ratio, (Höflich et al., 1998). Because of the lower energy production, the transition density is reached later in time, allowing for a longer expansion and then narrower region dominated by IME. One-dimensional delayed-detonation models have been successful in reproducing many observed characteristic of Type Ia supernovae but a complete description of the propagation of turbulent thermonuclear flame needs three-dimensional simulations. As pointed out by Gamezo et al. (2003) in a highly convoluted turbulent flame scenario the convective flows continuously take external material

to the interior of the star keeping an active burning in the inner layers of the expanding atmosphere. While the expansion proceeds the density decreases. Intermediate mass elements are formed for densities lower than $5 \cdot 10^7$ gr/cm^3 and the burning stops completly for densities lower than 10^6 gr/cm^3 The unburnt carbon and oxygen should then produce visible spectral features at different radii down to the center of the star. For an extensive review of the theoretical models and observations see (Hillebrandt et al., 2000; Leibundgut et al., 2000; Branch et al., 2001; Filippenko, 1997). From an observational point of view the conclusion that SNe Ia are the result of the explosion of carbon-oxygen white dwarfs is supported mainly on the absence of H lines. Prior light curve maximum normal type Ia SNe have spectra dominated by intermediate mass element such as SiII, SII, MgII, CaII and OI (Branch et al., 1993) and during the spectral evolution the absorptions due to this elements become weak and gradually more contaminated by iron-peak lines. The substitution is usually complete around 30 days after maximum when the supernova photosphere starts receding into the iron-peak core.

4. Spectra comparison

Objects such as SN1991T, SN1997br and SN2000cx, represent a deviation from the impressive homogeneity of the spectral and photometric characteristics of SN explosions (Fisher et al., 1999; Li et al., 1999, 2001a) and therefore have raised the question whether they could be explained as a different physical phenomenon or rather they must be considered as extreme cases of the same process. When SN1999aa was discovered and the first spectra circulated in the supernova community, the idea that this object could be helpful in addressing this question and that it could be used as a new supernovae prototype was proposed by several authors (Branch , 2001; Li et al., 2001b). This work should be viewed in that context.

4.1. Pre-maximum spectra

The spectra of SN1999aa and SN1991T are very different from the normal SNe 1990N and 1994D around 11 days prior to the B-band light curve maximum, as shown in Fig. 3. The identification of the lines labeled here and in the following graphs are taken from Li et al. (1999, 2001a); Fisher et al. (1999); Patat et al. (1996); Mazzali et al. (1995); Kirshner et al. (1993); Jeffrey et al. (1992). Instead of the typical SiII, SII and MgII lines early spectra of these peculiar SNe are dominated by two deep absorption due to FeIII $\lambda\lambda 4404, 5129$ Å . SiIII $\lambda 4560$ Å is responsible for the smooth absorption on the red side of the first FeIII line ($\lambda 4404$ Å) and smaller NiIII lines near $\lambda\lambda 4700$,5300, as pointed out by Jeffrey et al. (1992) and Ruiz-Lapuente et al. (1992). What mainly distinguish SN1999aa from SN1991T is the presence of the deep trough around 3800 Å, most probably CaII H&K even if much weaker compared to normals. On the red side of Ca H&K the small and not clearly defined absorption could be due to SiII $\lambda 4128$ Å and CoII $\lambda 4145$ Å , as in normals. The weak and broad line around 6150 Å could be due to SiII $\lambda 6355$Å with a contamination from CII $\lambda 6580$ Å as proposed by Fisher et al. (1999). The first time in which SiII $\lambda 6355$Å is clearly visible in our spectrum of SN1999aa is at -7 days, (Fig.2). By day -3, shown in Fig. 4, the spectrum goes through a big metamorphosis resembling more closely a normal Type Ia supernova. The intermediate mass elements start dominating the spectrum while in SN1991T the only signs of them are the CaII H&K and weak SiII lines in the 4000 Å and 6150 Å region respectively. The couple FeIII and SiIII $\lambda\lambda 4404, 4560$ Å are still intense and similar to those in SN1991T, the redder of the two Fe III is getting broader and flatter more like SN1994D. This is

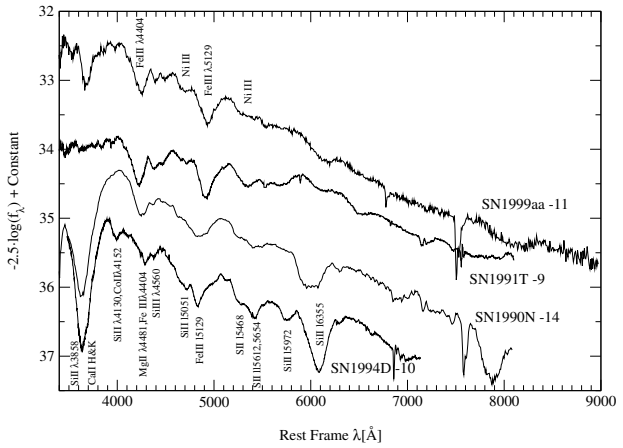

Fig. 3. The day -11 spectrum of SN1999aa together with of SN1991T, SN1990N and SN1994D from Richardson et al. (2002). Line identification is explained in the text.

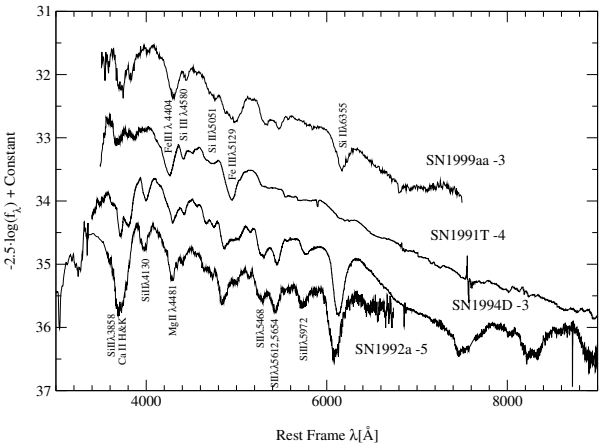

Fig. 4. The -3 spectrum of SN1999aa together with of SN1991T, SN1992A SN1994D from Richardson et al. (2002).

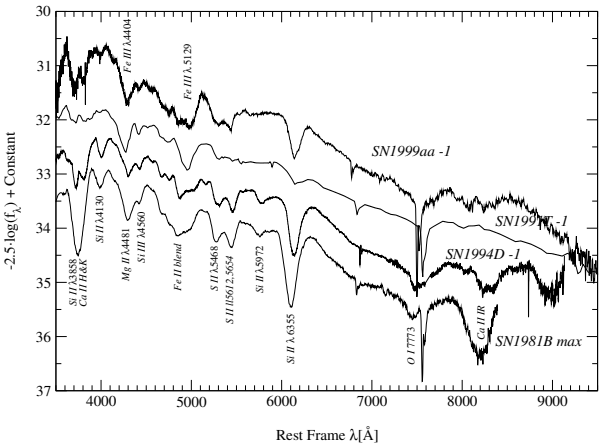

Fig. 5. The -1 day spectrum of SN1999aa together with of SN1991T, SN1981B and SN1994D from Richardson et al. (2002).

due to the contamination from FeII. SII appears strongly in this epoch showing the typical 'W' shaped feature at $\lambda\lambda 5454, 5606$ Å that SN1991-T like SNe do not show. The silicon line at $\lambda 6355$ Å is visible but fainter than in normals and much redder showing contaminations that will be more visible in the velocity time evolution of this line presented in the next section. SiII $\lambda 5958$ Å is still not evident. If the evolution from CII to SiII proposed by Fisher et al. (1999) can be confirmed, SN1991T at this epoch shows a much weaker absorption than SN1999aa, suggesting that the amount of Si present in SN1999aa is between that of normals and the truly peculiar over luminous as well as for Ca. SN1999aa already at this epoch appears generally much closer to normals compare to SN1991T or SN1997br, (see Fig.12 in Li et al., 1999).

4.2. Around maximum spectra

The spectrum around maximum shown in Fig. 5 resembles a normal Type Ia while SN1991T is still dominated by FeIII lines with very weak SiII and Ca H&K lines. The CaII H&K region shows the characteristic split with the contamination from SiII $\lambda 3858$ Å as proposed by Nugent et al. (1997) and Lentz et al. (2000), where the red component is gaining strength. No sign of SiII $\lambda 5972$ Å is present, confirming again the overall weakness of the IME layer in this object. The CaII IR triplet $\sim \lambda 8000$ Å has two weak wiggles not present in SN1981B but visible and deeper in SN1994D. All the other major features are the same seen in SN1994D; FeIII $\lambda 4404$ is still prominent and with an unchanged profile shape, on its red wing the SiIII it getting weaker while FeIII $\lambda 5129$ has been contaminated by the FeII. The spectrum of one week after maximum, Fig. 6, is completely normal, showing now also the blue component of the SiII duo in the 5700-6200 Å region while SN1991T (here at +9d) shows only weak SiII and SII lines, the latter

of which appears for the first time in the 'W' shaped λ5500 Å region. Unfortunately there is no data at precisely this epoch for SN1991T, but from +9d and from the spectra of 91T-like supernovae shown in (Li et al., 1999) and (Li et al., 2001a) it is clear that the general trend for this objects is to have still very weak intermediate mass elements components and a persistent dominant presence of highly ionized Fe, while in the normal SNe at this epoch iron-peak elements as CoII and FeII start to appear and CaII IR and OI λ7773 Å are getting stronger. The SII 'W' shaped in SN1994D and SN1990N is loosing definition and strength while in SN1999aa this is already at a more advanced stage. SN1999aa is very similar to normal Type Ias spectra at this epoch while, as reported in (Li et al., 1999) and (Li et al., 2001a) SN1997br and SN2000cx have an already massive contribution from low ionization iron-peak elements with SN1997br more advanced in this transition compared to SN1991T. This suggests a very interesting sequence among these objects in which the duration in the phase of the intermediate-mass elements is the shortest in SN1997br and the longest for SN1999aa with SN1991T placed somewhere in the middle. For Branch normal supernovae this phase extends from well before maximum to a couple of weeks after. In the case of these peculiar objects instead it seems to vary in duration and phase in the time evolution. This is probably due to the ratio Fe-peak/IME abundances and their radial distribution.

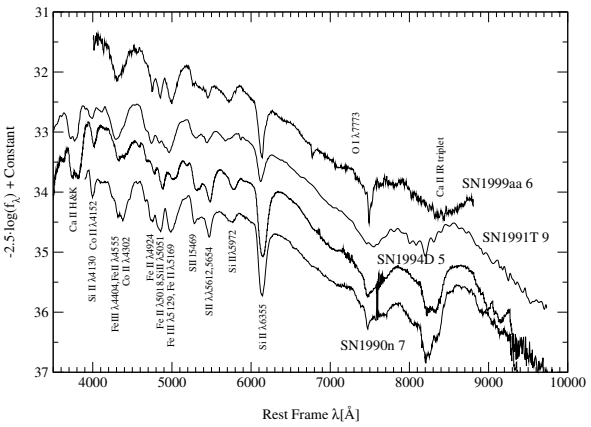

Fig. 6. The +6 day spectrum of SN1999aa spectrum together with of SN1991T, SN1990N SN1994D from Richardson et al. (2002).

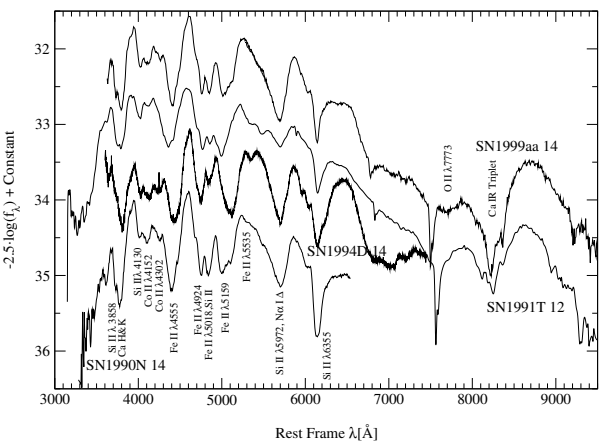

Fig. 7. The +14 day spectrum of SN1999aa spectrum together with of SN1991T, SN1990N and SN1994D from Richardson et al. (2002).

4.3. After maximum spectra

In the next set of spectra, shown in Fig. 7, SN1991T is still completing its intermediate mass elements phase with distinct P-Cygni profile for SiII λ6355 Å with virtually no contaminations from FeII. The 'W' of SII has not yet blended with NaI as in the other objects. The overall contribution of SII, SiII and CaII to its evolution is consistently weaker then in typical Type Ia. In SN1997br the bottom of SiII is flatted down by FeII lines (see Fig. 14 in Li et al., 1999). SN 1999aa is now completely indistinguishable from a normal supernova as SN1990N with maybe the only exception of a slightly fainter SiII λ6355 Å. Small differences are visible anyway also among normals. SN 1994D has a small absorption around 5500 Å that the other three objects do not show and that is maybe visible in SN1997br and identifiable as FeII λ5535 Å. As in the previous figure, the main differences at +25 days, Fig. 8, are around 6000 Å probably due to different Si abundance among the different objects. SN1991T here shows

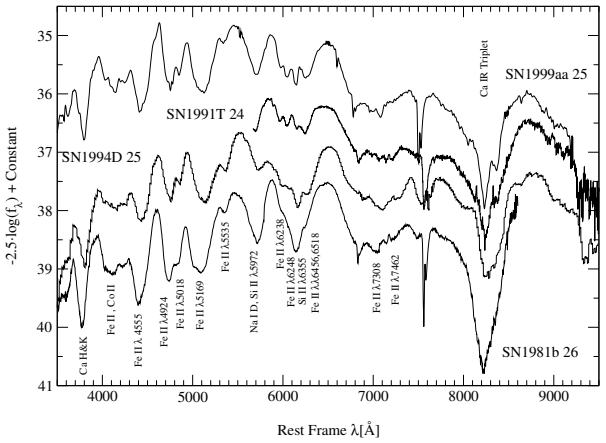

Fig. 8. The +25 day spectrum of SN1999aa spectrum together with of SN1991T, SN1981B and SN1994D from Richardson et al. (2002).

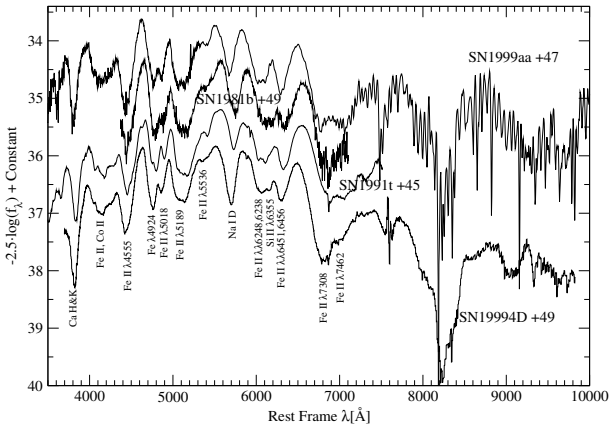

Fig. 9. The +47 day spectrum of SN1999aa spectrum together with of SN1991T, SN1981B and SN1994D from Richardson et al. (2002). The spectrum of SN1999aa is affected by fringing which has not been corrected for.

the FeII $\lambda\lambda 6238, 6246, 6456, 6516$ Å structures and just a very week SiII in the center while in SN1999aa the SiII is a bit more evident and it gets even stronger in SN1994D and SN1981B. The trough near 5700Å due to SiII $\lambda 5972$ Å and NaI D is strong in all the three SNe. At the very red end of the spectra the four objects show the typical Ca II IR triplet as a very deep and broad absorption, SN1999aa and SN1991T show a second minimum in the red part of this features. At this stage the spectra are all dominated by FeII and CoII lines showing that they are formed mainly in the deep layers of the atmosphere. Now, definitely in the nebular phase, Fig. 9 shows that differences are still visible at +47 days. SN1999aa is more similar to SN1994D than to SN1991T. In the $\lambda 4200$ Å region of the latter, two minima are visible and the red edge is flat. The absorption at $\lambda 4924$Å is deeper in SN1994D then in SN1999aa which has stronger Fe $\lambda 5536$ Å line. SN1994d has still a hint of Si II $\lambda 6355$ Å not present in SN1999aa and SN1991T but probably visible in the noisier spectrum of SN1981B. At the red end of the spectra of SN19994D and SN1999aa strong CA II IR triplet are visible. The spectrum of SN1999aa suffers from some fringing that has not been corrected in the reduction phase. Other small differences can be identified in the four spectra even at this epoch confirming that the overall evolution of the SN spectra has to be considered if we want really to understand the physics behind the peculiarities of the different objects.

5. Expansion Velocities

The expansion velocities as computed from fits to the minima of the lines can give help in investigating the physics of the supernova explosion. The weighted fit of the minima was done using a non-linear Marquard-Levemberg minimization procedure (Marquardt, 1963) applied on a Gaussian profile model. The minimum of the line was considered to be the center of the Gaussian and the fit uncertainty its statistical error. This is usually of the order of few km/s since the high signal to noise ratio of our data and thus is not shown on the graphs. For a quantitative study however the systematic uncertainties on the profile model chosen and on the wavelength range selected should be considered. The analysis presented in this work is not quantitative and thus the systematic uncertainties are not taken into account. The general trend for the fitting was to consider the entire absorption of the P-Cygni profile when this was not distorted too much by contaminations in which case a line sample closer to the bottom was taken

into account for the fit. In Figures 10-13 we show the velocities for CaII H&K, SiII (λ6355Å) and FeIII($\lambda\lambda$4404, 5129 Å) lines for SN1999aa and other several public supernovae. The CaII H&K velocities are in the normal range suggesting that if there is contamination from other elements (e.g SiIII, SiII, CoII) is not stronger then in other supernovae such as SN1994D. It is generally believed that the more energetic is the supernova explosion the more ^{56}Ni is produced and then more luminous the object should be. This would suggest that over luminous object should have higher velocities but no such correlation has been found (Hatano et al., 2000). For this line there is probably a trend to be a bit higher compare to normals. The SiII velocities are very interesting. If the absorption near 6150 Å was due only to SiIIλ6355 the velocities would have been monotonically decreasing with time as is clear for the normal SN1994D, SN1992A or for the sub-luminous SN1999by and SN1991bg. For SN1999aa the first point, 11 days before maximum light, has the lowest velocity, this is consistent with CII being the major responsible for this line at this epoch. The late time behavior is also interesting, the line minimum remain practically stable during the first 20 days after maximum. This is usually interpreted as if the element layer in the supernova atmosphere was confined in a region above the photosphere, in this case around $10000 km/s$. The same trend is shown by SN2000cx and SN1991T with a velocity close to $12000 km/s$ and $9300 km/s$ respectively, as shown in Fig.11 . The velocities measured for the two big FeIII features, dominant in the pre-maximum spectra of the peculiar over-luminous SNe and disappearing within the first week after maximum light, are also interesting. In both cases SN1999aa has the lowest velocities among SN1991T, SN1997br and SN2000cx but the same slope. Fe III λ4404Å velocities are smaller by 2500 km/s with respect to SN1991T and 3500 km/s with respect to SN2000cx. Fe III λ5129Å velocities are instead still smaller but much closer to the ones of the other peculiar supernovae. This could be due to a higher contamination from SiII λ5051Å or FeII λ5018Å . Generally the velocities ranges of SN1999aa line are quite consistent with a normal supernovae. The major peculiarity is the restricted atmosphere region in which SiII is present that makes clearly appear this ion only one week before maximum light.

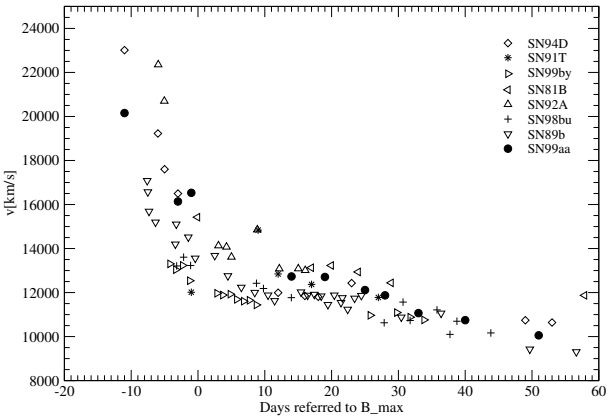

Fig. 10. Doppler shift of the Ca H&K line

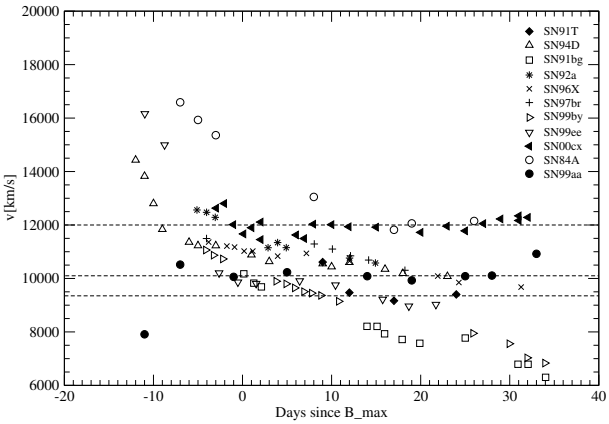

Fig. 11. Doppler shift of the SiII λ6350 Å line. Dashed lines indicating 12000 km/s, 10100km/s and 9350km/s.

6. Synthetic Spectra

In the previous sections we have taken an extensive look at the spectral features characteristics and evolution and enumerated the more evident differences in appearing among normal and peculiar supernovae and SN1999aa. Here we turn to a more quantitative analysis. We used

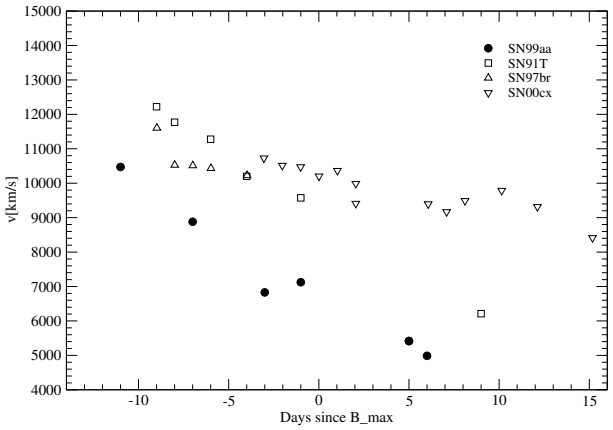

Fig. 12. Doppler shift of the FeIII λ4404 Å line

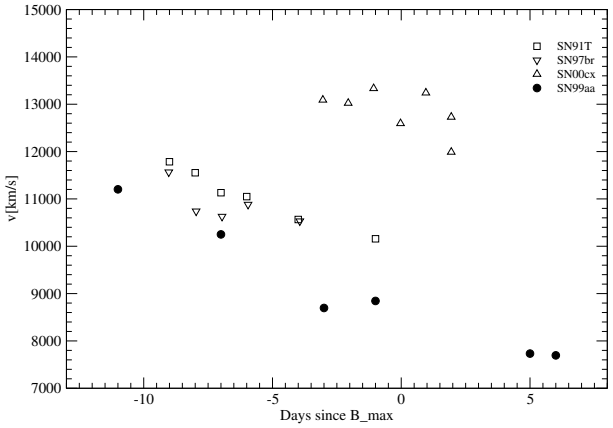

Fig. 13. Doppler shift of the FeIII λ5129 Å line

SYNOW, (Fisher et al., 1997, 1999), to produce synthetic spectra and to investigate line identification and velocities ranges. SYNOW is a highly parametrized supernova synthetic spectrum code that assumes a sharp photosphere in spherical symmetry and treats the line formation in the expanding supernova atmosphere in Sobolev LTE approximation and resonance scattering. The synthetic spectrum is computed considering the different selected ions and values of the input parameters. The parameters for each ion are: the velocity v_{phot} at which the photosphere is placed and below which the atmosphere is considered optically thick. The temperature, T_{bb}, for the black body continuum, the optical depth for the ion reference line τ and its velocity range v_{min} and v_{max}. For each ion the excitation temperature, T_{exc}, is input. The radial distribution of the

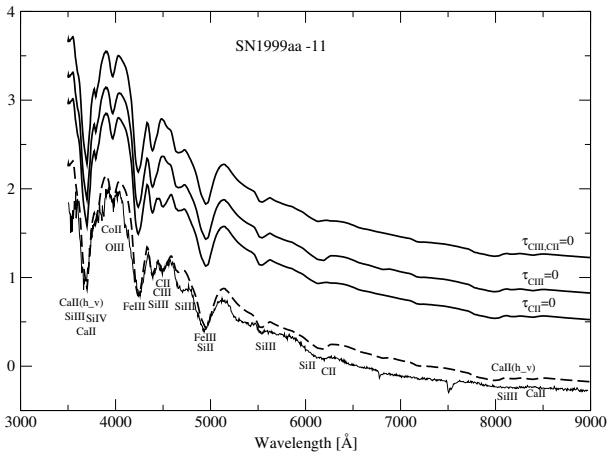

Fig. 14. Synthetic spectra compared with SN1999aa spectrum for day -11. Solid linee from top to bottom: $\tau_{CIII,CII} = 0, \tau_{CIII} = 0, \tau_{CII} = 0$, Dashed line: best match $\tau_{CIII,CII} \neq 0$

optical depth as a function of velocity (in the Sobolev approximation the expansion of the atmosphere is considered to be homologous) is considered exponential with e-folding velocity v_e. In the present modeling scenario with three dimensional asymmetric complete NLTE models, SYNOW can still give fast and useful information about the differences in the spectral composition and hints for the more rigorous hydrodynamical models. We have produced five synthetic spectra of SN1999aa for epoch 11, and 1 before maximum light and 5, 14, 40 after.

6.1. -11 Days

In Fig. 14 we show the results for the best match synthetic spectrum computed using the parameters in table 2 togheter with the results exluding the CII and CIII components. The continuum black body temperature is 13700 K and the photosphere is placed at 11000 km/s. The only way we found to account for the complete structure of the CaII H&K features and for its velocity distribution (blue edge at 40000 km/s) is to introduce a high velocity component in addition to the one at v_{max}=20000km/s. At this epoch this allows us to 'fill-up' the whole spectral profile and at later epochs it will produce the observed

blue wiggle of the CaII IR triplet as noticed already in Hatano et al. (1999b) for SN1999D. The other dominant features at this epoch are the two big FeIII lines, the first of which ($\sim \lambda$4250 Å) needs an important contribution from OIII in order to have the observed strength and minimum wavelength. The small absorption around 4000 Å is identified as CoII. Note that in order to have the red edge and the minimum matching the data this ion needs to be detached from the photosphere. SiIII is responsible for the feature at 4400 Å and 5500 Å as well as for the one at 4700 Å as identified by Jeffrey et al. (1992). SiIV is useful to match the data in the 3900 Å region. The features at 6150Å has a very broad profile, to reproduce it the usual SiII plus CII at high velocities have been used. As shown in Fig. 14 in absence of the C component and using only SiII the feature would look to blue and with the usual P-Cygni profile. In spite of trying many other possibilities, no other ion has shown a convincing contribution at this wavelengths. In the spectral time sequence, Fig. 2, we can see that shape of this line changes at -7 days with the appearance of the first strong SiII λ6355 line at the right velocity, (Fig. 11). The feature at 4500 Å is formed by a blend of CII and CIII. The identification of CII, CIII and OIII favor the presence of an unburned region of C+O rich composition, as shown in Fig. 5 in (Hatano et al., 1999a). The identification of an external layer of carbon has been proposed originally by Fisher et al. (1997) and re-proposed for SN1991T by Fisher et al. (1999) based on the possible presence of the CII line on the SiII λ6355 Å region. In our spectrum of SN1999aa we clearly identify a second absorbtion mainly due to CIII λ4648.8Å on the red of SiIII λ4568 Å . Its importance for a good match of the observed spectrum is shown in Fig. 14 where a series synthetic spectra with and without C components are compared with SN1999aa at 11 day before maximum. The line identifications for this spectrum

Ion	τ	v_{min}	v_{max}	T_{exc}	v_e
		$10^3 \mathrm{km s}^{-1}$	$10^3 \mathrm{km s}^{-1}$	10^3K	$10^3 \mathrm{km s}^{-1}$
CaII	0.6	-	19	15	5.5
CaII	1.1	19	70	15	6.5
SiII	0.1	-	20	15	5
SiIII	0.65	12.7	15	22	3
SiIV	0.2	0	30	15	5
CoII	0.2	15	17	10	3
FeIII	0.65	-	23	10	3
CII	0.015	19	50	15	5
CIII	0.3	-	14.5	15	4
OIII	1	-	20	15	3

Table 2. Synow parameters for day -11. Vphot=11000km/s, $T_{bb} = 13700$

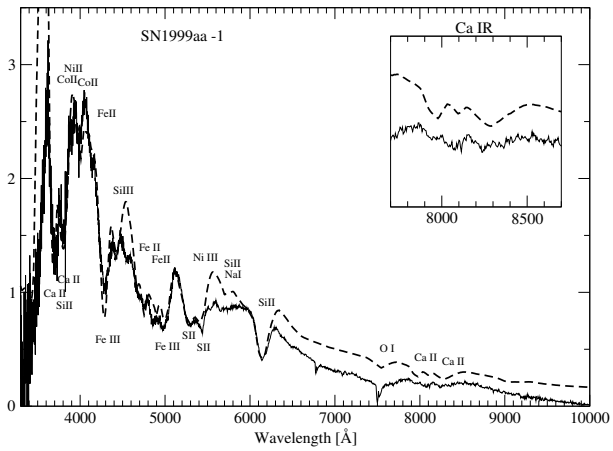

Fig. 15. Synthetic spectrum compared with SN1999aa spectrum for day -1. The inset graph shows the velocity range match in the CaII IR triplet region.

are consistent with a peculiar object but show a very interesting CaII not present in the other objects of the same kind.

6.2. -1 Days

By day -1, the spectrum as shown in Fig. 15 looks much more similar to normal Type Ias but the synthetic spectrum input parameters show a dominance of features due to heavy elements; see details in table 3. The optical depth

Ion	τ	v_{min}	v_{max}	T_{exc}	v_e
		$10^3 \mathrm{km} s^{-1}$	$10^3 \mathrm{km} s^{-1}$	10^3 K	$10^3 \mathrm{km} s^{-1}$
CaII	3	-	18	5	6
CaII	2.5	21	25	5	5
OI	0.2	-	30	5	3
SiII	1.	-	15	10	3
SiIII	0.6	10	25	10	6
SII	0.6	10	25	10	6
FeII	0.5	17	40	8	5
CoII	0.2	15	20	10	3
NaI	0.3	10	45	8	4
FeIII	0.5	-	12.5	6	3
NiIII	15	-	12	13	3
NiII	0.05	-	35	5	3

Table 3. Synow parameters for day -1. Vphot=9000km/s, $T_{bb} = 13500$

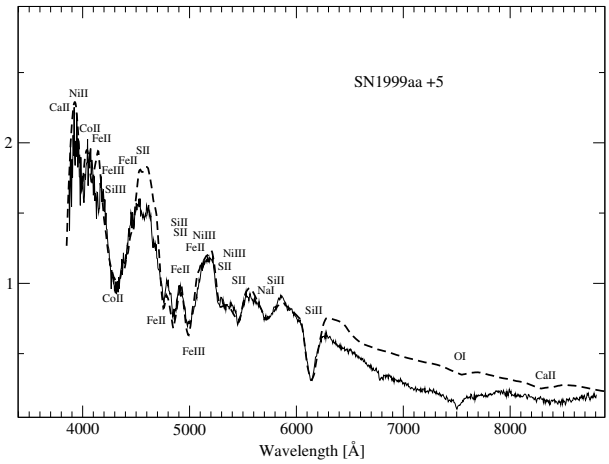

Fig. 16. Synthetic spectrum compared with SN1999aa spectrum for day +5

of ions such as FeII, CoII, and NiII are greater than those for the typical SiII and SII characteristic of the Branch-normal supernovae. The presence of highly ionized elements (FeIII, SiIII, NiIII) still make an important contribution, showing that the temperature in the atmosphere is still high. The need for double layers of CaII is evident at this epoch both in the H&K and IR triplet regions. The only way we found to account for the two small wiggles in the blue part of the CaII IR triplet is to include an higher velocity component as shown in the inset graph of Fig.15. The black body continuum does not match the observed spectrum above 6300 Å but nevertheless the two minima of the high velocity component of CaII IR triplet are well constrained. In order to achieve a better match a 3D treatment would be needed as shown in Thomas et al. (2003).

6.3. +5 Days

In the synthetic spectrum produced for +5 days, as shown in Fig. 16, we still find useful to introduce lines from NiIII, SiIII and FeIII but with lower τ; see table 4. The main contribution of NiIII is in lowering the emission between the two SII features at 5400 Å. FeIII and SiIII help in forming the big trough at 4400 Å together with FeIII and CoII. The feature at 5700 Å is composed mainly of NaI, the SiII component results to be weak thanks to the low excitation temperature at which has been introduced; a higher temperature would create a redder features than the one seen in the data. In order to reproduce the three distinct minima below 5000 Å , the FeII layer has to be detached and shallow in velocity space, otherwise the lines tend to blend together forming a single broad feature as seen in SN1981g. Unfortunately our spectra doesn't cover the region below 3900 Å and the Ca IR triplet is too weak to fully determine whether there is still need for a high velocity CaII component.

Ion	τ	v_{min}	v_{max}	T_{exc}	v_e
		10^3kms^{-1}	10^3kms^{-1}	10^3K	10^3kms^{-1}
CaII	10	-	50	5	3
OI	0.1	-	30	5	3
SiII	1.5	10	15	5	3
SiIII	0.3	16	40	5	3
SII	0.5	10	13	8	3
FeII	1.5	11	15	5	3
CoII	0.8	13	40	5	3
NaI	0.4	0	17	5	3
FeIII	0.09	-	30	5	3
NiIII	8	-	13	13	3
NiII	0.1	-	40	3	10

Table 4. Synow parameters for day +5. Vphot=9000km/s, $T_{bb} = 12000$

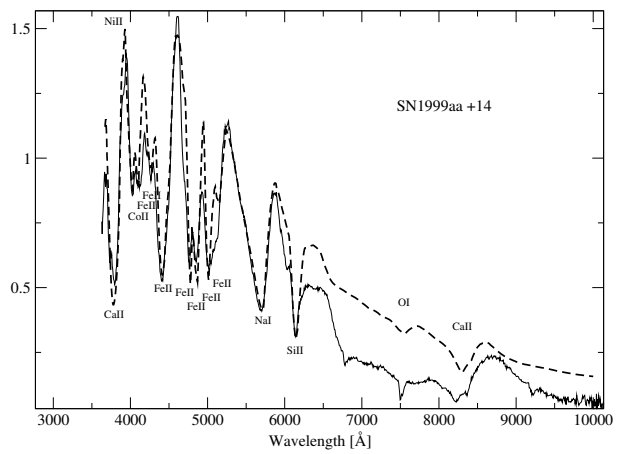

Fig. 17. Synthetic spectrum compared with SN1999aa spectrum for day +14

6.4. +14 Days

In the synthetic spectrum at day +14, shown in Fig. 17, FeII appears to be already the dominant ion; see table 5. NaI has blended with SII, due to the value of $v_{max} = 35$ km/s . As at the previous epoch, in order to reproduce the three different minima in the FeII blend region we use a minimum velocity higher than that of the photosphere. During the whole spectral evolution the region between 6500Å and 8000Å has become increasingly more and more difficult to match. At this epoch the discrepancy between data and synthetic spectrum are fairly evident. This is probably due to the increasing inaccuracy of the black body continuum assumption.

Ion	τ	v_{min}	v_{max}	T_{exc}	v_e
		10^3kms^{-1}	10^3kms^{-1}	10^3K	10^3kms^{-1}
CaII	20	-	45	8	3
OI	0.1	-	30	5	3
SiII	1.5	10	14	8	3
FeII	5	9.5	13.5	5	2
CoII	1.6	10	20	7	3
NaI	1.2	0	35	5	5.5
NiII	3	-	10	5	5

Table 5. Synow parameters for day +14. Vphot=8500km/s, $T_{bb} = 10500$

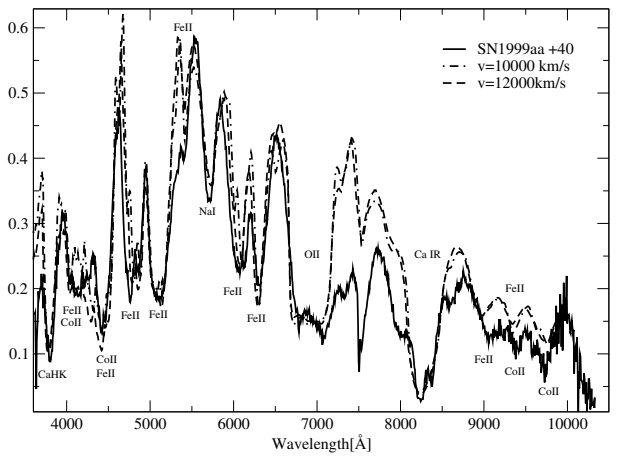

Fig. 18. Synthetic spectrum compared with SN1999aa spectrum for day +40. Dashed line max velocity for Fe-peak core at 12000 km/s. Dotted-Dashed line max velocity for Fe-peak core at 9000 km/s

6.5. +40 Days

Deeply into the iron-group core, at +40 days the supernova spectrum is mainly formed by FeII and CoII. The only signs of IME are CaII H&K and IR. A strong and wide feature near 7000Å can be reproduced by a forbidden line of OII with a very high v_e. For the details of

Ion	τ	v_{min}	v_{max}	T_{exc}	v_e
		10^3kms^{-1}	10^3kms^{-1}	10^3K	10^3kms^{-1}
CaII	300	-	18	8	3
OII	0.1	-	30	10	20
FeII	70	0	12	7	6
FeII	0.2	12	50	7	3
CoII	30	0	12	7	3
CoII	0.4	12	50	7	6
NaI	0.6	7	45	5	6

Table 6. Synow parameters for day +40, high velocity Fe-peak core. Vphot=7000km/s, T_{bb} = 8000

Ion	τ	v_{min}	v_{max}	T_{exc}	v_e
		10^3kms^{-1}	10^3kms^{-1}	10^3K	10^3kms^{-1}
CaII	300	-	17	8	3
OII	0.1	-	30	10	20
FeII	70	0	10	7	6
FeII	1.3	10	50	7	5
CoII	45	0	10	7	3
CoII	0.8	10	50	7	5
NaI	0.6	7	45	5	6

Table 7. Synow parameters for day +40, low velocity Fe-peak core. Vphot=7000km/s, T_{bb} = 8000

the composition see table 6. Some consideration has to be made about the way the components of FeII and CoII have been introduced. At this epoch the spectrum is formed into the Fe-peak core but still a part of the outer atmosphere makes a contribution. The optical depth of these elements in these two regions can in principal be different. We find useful to introduce a double layer of Fe and Co with different τ. The velocity at which this change occurs can be thought to be the iron peak core limit. Although several attempt to find the best match, it is not evident how much better an higher (12000 km/s) velocity limit fits the data with respect to a lower one (10000 km/s) (details in table 7). The two synthetic spectra are shown in fig 18. A definitive word cannot be said on this issue even if a more extended iron-peak is probably slightly favored.

7. Summary

Based on the current understanding of supernova physics and on the result presented in this work we can try to suggest a possible model for describing the observable characteristics of SN1999aa. As pointed out in (Nugent et al., 1995) the presence of highly ionized Fe and Si in the early spectra suggests higher temperature than in Branch normal SNe (see e.g. Hatano et al., 1999a, Figure 7). As shown in Figs 12 and 13, FeIII lines do not appear to be formed at very high velocities, (< 12000 km/s). Thus, SN1999aa does not necessarily require a more powerful explosion and a higher production of ^{56}Ni. In velocity space this is consistent with an oxygen burning composition in the W7 model. From the velocities inferred for CII and CaII H&K for the pre-maximum synthetic spectrum it appears that a C+O rich external layer is present at $v > 17000$ km/s. A similar conclusion is presented in (Fisher et al., 1999) where they introduced CII at $v > 15000$ km/s for SN1991T. The presence of this ion is indispensable to explain the line shape and velocity time evolution of the feature at 6150 Å for SN1999aa, as shown in Fig. 11. In this work we present the evidences for the identification of a CIII line λ4648.8 Å at photosphere velocities. The presence of unburnt material deep into the IME's atmosphere region is expected in 3D models where convective flows are shown to keep refueling the inner layers with original composition at high velocity as the expansion proceeds. The time evolution of the Doppler blue-shift of SiII around and after B maximum shows that this layer is confined within a thin velocity range, not only for SN1999aa but also for SN1997br, SN2000cx and SN1991T. Independent evidence for SN1999aa is given by the SYNOW spectra were veloc-

ities between 10000 km/s and 15000 km/s where needed to match the observations when the photosphere velocity dropped below 9500 km/s; see table 3. The velocity distribution for other IME's is similar to that of SiII. The same holds for SN1997br (Hatano et al., 2002) and for SN1991T (Fisher et al., 1999). No SYNOW synthetic spectra are available for SN2000cx but from the minima of the lines it seems to be formed in a slightly higher velocity layer; that velocity is stable around 12000 km/s. For a normal Type Ia supernova, such as SN1994D, the Si rich layer extends out to 27000 km/s. The presence of NiIII and the absence of CoIII lines seem inconsistent with these ions coming from a nickel decay composition. The innermost layers of W7 are considered to have gone through complete silicon burning, leaving only a nuclear statistical equilibrium composition such as shown in Hatano et al. (1999a, Fig. 9). The decay of the resulting ^{56}Ni to ^{56}Co and to stable ^{56}Fe would imply the presence of CoIII lines. In agreement with Hatano et al. (2002), we suggest that these lines are produced by ^{54}Fe and ^{58}Ni synthesized during incomplete and complete silicon burning. If this is the case, it is not required to produce a model that extends the complete silicon burning in the region of intermediate mass elements or above, as originally proposed for SN1991T-like objects. Among the current DDT models it seems that none is able to extend the presence of this ions as far out as is thought to be necessary to match the observations ($v_{max} > 20000$ km/s table 2). However, Höflich et al. (1998) showed that a higher initial metallicity would increase the abundance of ^{54}Fe and ^{58}Ni and this could possibly explain the observations. UV photometry and spectroscopy would yield important information to settle this issue (Lentz et al., 2000). The iron peak core composition can be investigated using late spectra. In the synthetic spectrum produced for +40 days, Fig. 18, we found that a limit velocity ~ 12000 km/s for the Fe-peak core is probably favored compared to 10000 km/s.

8. Conclusions

We have presented detailed analysis of the spectrum development of SN1999aa. The overall evolution of spectral features suggests a peculiar over-luminous object with a hot exterior and possible signs of high metallicity. The line identification for the earliest spectrum shows a carbon layer and highly ionized ions consistent with C+O rich composition. The identification of CIII λ4648.8 Å at photosphere velocity, if confermed, shows the presence of original unburnt material in the IME's region of the atmosphere. The spectral evolution of SN1999aa shows that IME's populate a narrow velocity window. Similar evidences are found in other well known peculiar supernovae explosions (e.g. SN1991T, SN1997br and SN2000cx). The iron peak core extends further out and dominates the spectra at larger radii than in normals. The comparison with other peculiar objects of the same kind suggests that the transition between IME to iron-peak dominant composition can occur at slightly different times. The real origin of the differences between normal supernovae and peculiars probably depends on several factors. The increasing of the temperature has been shown to be able to account for some of the peculiarities (Nugent et al., 1995). Higher temperatures in the outer layers implies more powerful explosion, more ^{56}Ni, more luminous events and higher expansion velocities. This is clearly not an adequate explanation. Examples such as SN1984A, with normal looking spectra and light curve but higher expansion velocities (Lentz et al., 2001a), or SN1991T, (Fisher et al., 1999, and references therein) over luminous and spectroscopically peculiar but with average expansion velocities are convincing examples showing that our understanding of SNe Ia is still incomplete. Iwamoto et al. (1999) pre-

sented a model (CS15DD3) with ^{58}Ni and ^{54}Fe extending to higher velocities and with the presence in the same region of intermediate mass elements. As already proposed for SN1997br by Hatano et al. (2002) this is consistent with the observed and synthetic spectra presented here for SN1999aa, but does not explain the lack of correlation between velocities and luminosity.

New accurate optical and infrared spectra as well as spectro-polarization studies are needed to support the evolving degree of complexity of the models proposed and to give a complete explanation of the physics of supernovae explosions. SN1999aa provides clear evidence, however, that perhaps a single model could explain both normals and peculiar SN1991T-like SNe and that this object might be positioned between the two extremes on a single class of events.

References

Aldering, G. 2000, "Type Ia Supernovae & Cosmic Acceleration," *AIP Conference Proceeding: Cosmic Explosions*, ed. S. S. Holt & W. W. Zhang, Woodbury, New York: American Institute of Physics.

Arbour, R. 1999, IAU Circ. 7108

Branch D., Fisher A., Nugent P., 1993, AJ 106, 2383.

Branch D. 2000 astro-ph/0012300

Branch D, Baron E. Jeffery J. D. astro-ph/0111573

Branch D, 2001 PASP,113,169B

Cardelli J. A., Clayton G. C., Mathis J. S., 1989, ApJ, 345, 245.

Filippenko Alexey V. 1992 ApJ, 384, L15.

Filippenko Alexey V. 1997 ARA&A, 35, 309F.

Filippenko, A. V., Li, W. D., Leonard, D. C. 1999, IAU Circ. 7108

Fisher A., Branch D., Hatano K., Baron E., 1999, MNRAS, 304, 67-74.

Fisher A., Branch D., Nugent P., Baron E., 1997, ApJ, 304, L89

Folatelli et al. 2003, in prep.

Folatelli et al. 2003, in prep.

Gamezo Vadim N., Khokhlov Alexei M., Oran Elaine S., Chtchelkanova Almadena Y., Rosenberg Robert O. 2003 Sci, 299, 77G.

astro-ph0105490

Goobar A., Perlmutter S., 1995, ApJ, 450, 14.

Hatano K., Branch D., Fisher A., Millard J., Baron E., 1999, ApJ, 121, 233.

Hatano K et al., 1999, ApJ, 525, 881-885.

Hatano K.,Branch D.,Lentz E.J.,Baron E.,Filippenko A. V., 2000, ApJ, 543, L49.

Hatano K., Branch D., Qiu Y.L., Baron E., Thielemann F.-K., 2002, NewA, 7, 441.

Hillebrandt et al ARAA 2000, 38, 191.

Horne, K. 1986, PASP, 98, 609

Höflich P., 1995, ApJ, 443, 89-108.

Höflich P., Wheeler J. C.,Thielamann F.-K., 1998, ApJ, 495, 617.

Iwamoto K., Brachwitz F., Nomoto K., Kishimoto N., Umeda H., Raphael Hix W., Thielemann F-K., 1999, ApJS, 125

Jeffrey D. J., Leibundgut , Kirshner R. P., Benetti S., Branch D. & Sonnenborn G., 1992, ApJ, 397, 304.

Khokhlov A.M., 1991, A&A, 245, 114.

Kirshner R. P. et al 1993 ApJ, 415, 589.

Krisciunas K., Hastings N.G., Loomis K., McMillan R., Rest A., Riess A. G., Stubbs C., 2000 ApJ, 539, 658.

Leibundgut et al AAR 2000, 10, 179.

Lentz E.J., Baron E., Branch D., Hauschildt P.H.,Nugent P., 2000, ApJ, 530, 966-976.

Lentz E.J., Baron E., Branch D., Hauschildt P.H. 2001 ApJ, 547, 402L.

Lentz E.J., Baron E., Branch D., Hauschildt P.H., 2001, ApJ, 557, 266-278.

Lentz E.J., Baron E., Branch D., Hauschildt P.H., 2001, ApJ, 547, 402.

Li W.D. et al. 1999 ApJ 117, 2709-2724.

Li W.D. et al. 2001, PASP, 113, 1178-1204.

Li W. et al. 2001, ApJ, 546, 724.

Marquardt Donald W.,J. Soc. Indust. Appl. Math. Vol. 11. No. 2, June 1963

Mazzali P.A, Danzinger I.J., Turatto M.. 1995 A&A, 297, 509-534.

Mazzali Paolo A. 2001 MNRAS, 321, 341-346.

Nakano, S., Kushida, R. 1999, IAU Circ. 7109

Nomoto K., Thielemann F.-K., Yokoi K. 1984, ApJ, 286, 644.

Nugent, P., Aldering, G., & The Nearby Campaign 2000, Supernovae and gamma-ray bursts: The Greatest Explosions Since the Big Bang: poster papers from the Space Telescope Science Institute Symposium, May 1999 / Mario Livio, Nino Panagia, Kailash Sahu, editors. [Baltimore, Md.] : Space Telescope Science Institute, [2000]., p.47, 47.

Nugent P.,Baron E., Branch D., Fisher A., Hauschildt P.H, ApJ 485, 812-819.

Nugent P., Phillips M., Baron E., Branch D., Hauschildt P.H, ApJ 455, 147.

Patat et al. 1996, MNRAS, 278, 111-124.

Prlmutter et al. 1999, ApJ, 517, 565

Phillips et al. 1999, AJ, 118, 1766

Qiao, Q. Y., Wei, J. Y., Qiu, Y. L., Hu, J. Y. 1999, IAU Circ. 7109

Richardson, D.; Thomas, R.; Casebeer, D.; Branch, D.; Baron, E. 2002 AAS, 201, 5609R

Riess et al. 1998, AJ, 116, 1009

Ruiz-Lapuente P., Cappellaro E., Turatto M., Gouiffes C., Danziger I. J., della Valle M., Lucy L. B., 1992ApJ, 387L, 33R.

Schlegel, D. J., Finkbeiner, D. P., Davis, M. 1998, ApJ, 500, 525

Thomas R. C., Branch D., Baron E., Nomoto K., Li W., Filippenko A. V., 2003, astro-ph/0302260

Woosley S. E., Weaver T. A., 1986 ARA&A 24, 205.

Yamaoka H., Nomoto K., Shigeyama T., Thielamann F.-K., 1992, Apj, 393,55.